Vol 17 No 9, September 2008
1674-1056/2008/17(09)/3422-06

Chinese Physics B

© 2008 Chin. Phys. Soc.
and IOP Publishing Ltd

First-principles study of interphase Ni_3Sn in Sn–Ni alloy for anode of lithium ion battery*

Hou Xian-Hua(侯贤华)[a], Hu She-Jun(胡社军)[a)b)†], Li Wei-Shan(李伟善)[c)‡],
Ru Qiang(汝　强)[a], Yu Hong-Wen(余洪文)[a], and Huang Zhao-Wen(黄钊文)[a]

[a] *School of Physics and Telecommunication Engineering, South China Normal University, Guangzhou* 510006, *China*
[b] *Department of Mathematics and Physics, Wuyi University, Jiangmen* 529020, *China*
[c] *Department of Chemistry, South China Normal University, Guangzhou* 510006, *China*

(Received 3 January 2008; revised manuscript received 23 February 2008)

This paper investigates the mechanism of Li insertion into interphase Ni_3Sn in Ni–Sn alloy for the anode of lithium ion battery by means of the first-principles plane-wave pseudopotential. Compared with other phases, it is found that the Ni_3Sn has larger relative expansion ratio and lower electrochemical potential, with its specific plateaus voltage around 0.3 eV when lithium atoms are filled in all octahedral interstitial sites, and the relative expansion ratio increasing dramatically when the lithiated phase transits from octahedral interstitial sites to tetrahedral interstitial sites. So this phase is a devastating phase for whole alloy electrode materials.

Keywords: Sn–Ni alloy, first-principle, electronic structure, lithium ion battery

PACC: 7115A, 8640H

1. Introduction

Li rechargeable batteries have become one of the most developing power sources in the 21st century.[1−3] The demand for lithium ion batteries as a power supply for portable electric devices has continuously increased, but the lithium insertion capacity of graphite, the anode of commercial lithium ion battery, has already reached the theoretical limitation ($372\,\mathrm{mA\cdot h/g}$ as C_6Li). In order to enhance the energy density of lithium ion batteries, new anode materials need to be developed.[4,5]

It is regarded that tin is good for the anode of lithium ion battery to replace graphite because of its superior lithium storage capacity ($994\,\mathrm{mA\cdot h/g}$ as $Li_{4.4}Sn$).[6] The main issue to limit the commercialization of tin lies in the large initial irreversible capacity fades and relatively large volume expansion that lead to mechanical disintegration of the electrode. In order to reduce this irreversible capacity loss and alleviate the volumetric change, the combination of active and inactive components is found to be effective.[5,7] The inactive component can buffer the volume change caused by the active component, so as to improve the cycling performance of electrode. However, there are various interphases between active and inactive components, consequently it is necessary to understand their influences on electrochemical properties to get best performance of Sn alloy electrode.

First-principle calculations have made an impact on the understanding of practical lithium-ion battery materials.[8−11] For example, Xu *et al*[12] and Tang and Holzwarth[13] calculated and compared the electronic structures of $LiFePO_4$ and $FePO_4$. Courtney *et al*[14] calculated the voltage profile of lithium-tin alloy. They shows that the theoretical results agree with the corresponding experiments very well. In this paper, lithium insertion mechanism and electronic structure of interphase Ni_3Sn in Sn–Ni alloy as anode of lithium ion battery were investigated by using first-principle plane-wave pseudopotential method.

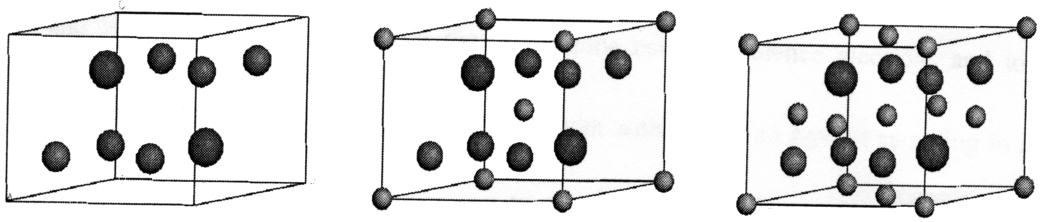
*Project supported by the National Natural Science Foundation of China (Grant No 50771046), the Key Program of Natural Science Foundation of Guangdong Province of China (Grant No 05200534), the Program for Tackling Key Problems of Guangdong Province of China (Grant No 2006A10704003) and the Program for Tackling Key Problems of Guangzhou City of China (Grant No 2006Z3-D2031).

†E-mail: husj@scnu.edu.cn
‡E-mail: liwsh@scnu.edu.cn

2. Structure and computational method

2.1. Structure model

The interphase Ni_3Sn is a hexagonal cell in Sn-Ni alloy, its space group is $P63/mmc$, with experimental lattice parameters $a = 0.5275\,\text{nm}$ and $c = 0.4234\,\text{nm}$. The unit cell is depicted in Fig.1(a). The reaction of lithiation/delithiation occurs during the process of charge and discharge, the lithium atoms inhabit the octahedral and tetrahedral interstitial sites of the host material Ni_3Sn. In this paper, it is assumed that the lithium atoms firstly fill the octahedral sites and then the tetrahedral sites when the octahedral sites are all taken. Two specific structures of lithiated Ni_3Sn are shown in Fig.1(b) (octahedral occupation) and Fig.1(c) (octahedral and tetrahedral occupation).



(a) Ni_3Sn (b) $LiNi_3Sn$ (c)$Li_{2.5}Ni_3Sn$

Fig.1. The crystal structure of Li_xNi_3Sn with $x = 0$ (a), 1 (b), 2.5 (c), respectively.

2.2. Computational details

The calculations are based on density-functional theory (DFT) with the plane-wave pseudopotential method. According to DFT,[15−19] the Schrödinger equation of single electron is

$$\left[-\frac{\nabla^2}{2m} + V_{\text{ext}}(\boldsymbol{r}) + V_{\text{xc}}(\boldsymbol{r}) + V_{\text{eff}}(\boldsymbol{r}, \rho(\boldsymbol{r}))\right]\phi_n(\boldsymbol{r}) = \varepsilon_{\text{i}}\phi_n(\boldsymbol{r}), \tag{1}$$

$$\rho(\boldsymbol{r}) = \sum_n a_n \left|\phi_n(\boldsymbol{r})\right|^2. \tag{2}$$

In equation (2), $\rho(\boldsymbol{r})$ is the density of electron states in system, and $\phi_n(\boldsymbol{r})$ is plane wavefunction of an electron. The first part of equation (1) is effective kinetic energy. The second part $V_{\text{ext}}(\boldsymbol{r})$ is external field potential. The third part $V_{\text{xc}}(\boldsymbol{r})$ is the exchange correlation potential. The final part $V_{\text{eff}}(\boldsymbol{r}, \rho(\boldsymbol{r}))$ is effective potential, and it can be written as

$$V_{\text{eff}}(\boldsymbol{r}, \rho(\boldsymbol{r})) = V_{\text{comb}}(\boldsymbol{r}) + \phi(\rho(\boldsymbol{r})), \tag{3}$$

where $V_{\text{comb}}(\boldsymbol{r})$ is the coulomb potential, it consists of norm-conserving pseudopotential and ultrasoft. $V_{\text{comb}}(\boldsymbol{r}) = \sum_N \dfrac{Z_N}{|\boldsymbol{r} - R_N|}$. $\phi(\rho(\boldsymbol{r}))$ is coulomb potential between electrons, which is defined as $\phi(\rho(\boldsymbol{r})) = \int \dfrac{\rho(\boldsymbol{r}')}{|\boldsymbol{r} - \boldsymbol{r}'|}\mathrm{d}\boldsymbol{r}'$. In this paper, all the calculations were completed with Cambridge serial total energy package (CASTEP). The calculations are based on DFT with the general gradient approximation using Perdew–Wang (PW91) form for the exchange correlation energy.[20] The ultrasoft Vanderbilt-type pseudopotentials[21] supplied by Kresse and Hafner are used to describe the interactions between valence electrons and ions. Calculations were converged to within 0.2 meV per atom with respect to k-point sampling in the Brillouin zone and the number of plane-wave basis functions (for the primitive unit cell of Li_xNi_3Sn, a $4 \times 4 \times 5$ Monkhorst–Pack[22,23] mesh and an energy cut-off of 300 eV were used). The ionic positions, lattice parameters, and cell volume are all relaxed with the conjugated gradient method using forces and stresses. The geometry optimization was stopped when all relaxed forces are less than 0.005 eV/nm. The maximum displacement error is within 0.005 nm and the maximum stress was less than 0.1 GPa.

3. Results and discussion

3.1. Total-energy calculations applied to electrochemistry

Several groups have recently performed first-principle calculations of various electrode materials. Courtney *et al*[14] calculated the voltage profile and energy density for lithium–tin alloy. Aydinol *et al*[24] calculated the average voltages for $Li/LiMO_2$ and

Li/LiCoX_2 (M = Ti, V, Mn, Co, Ni, Cu, Zn, Al; X = O, S, Se) cells. An approximation made in these calculations is that the transformation from reactant to product is two phases, and so an average voltage can be defined. In this paper, the reaction is assumed to be

$$Ni_3Sn + x\text{Li} \rightarrow \text{Li}_x\text{Ni}_3\text{Sn}. \quad (4)$$

The total energy calculations for $\text{Li}_x\text{Ni}_3\text{Sn}$, lithium metal and Ni_3Sn are listed in Table 1. Therefore, in order to obtain the difference of total energy (ΔE) for the insertion reaction, we use the following equation:

$$\Delta E = [E_{\text{total}}(\text{Ni}_3\text{Sn}, V_0) + xE_{\text{total}}(\text{Li}) - E_{\text{total}}(\text{Li}_x\text{Ni}_3\text{Sn}, V)]. \quad (5)$$

In Eq.(5), E_{total} (Ni_3Sn, V_0) and E_{total} ($\text{Li}_x\text{Ni}_3\text{Sn}$, V) are the total energy per formula unit of Ni_3Sn and $\text{Li}_x\text{Ni}_3\text{Sn}$, respectively. E_{total} (Li) is the total energy of metallic lithium. However, the theoretical procedure to calculate the average insertion voltage through first-principles has already been established. The insertion voltage is given by[25]

$$\bar{V}(x) = -\Delta G/x, \quad (6)$$

here ΔG is the change of Gibbs free energy for the insertion reaction and x is the charge transported by lithium in the electrolyte. Assuming that the changes in volume and entropy associated with the insertion are negligibly small, we can approximate ΔG can be approximated by the internal energy term ΔE, so equation (6) can be written as follow

$$\bar{V}(x) \approx -\Delta E/x. \quad (7)$$

Meanwhile, it is assumed that V_0 and V is the equilibrium volumes before and after insertion reaction, so the coefficient of relative expansion is defined as

$$\Delta V = \frac{V - V_0}{V_0} \times 100\%. \quad (8)$$

According to the relation of weight capacity and the empirical law, the calculated specific capacity is defined as:

$$C_{\text{cal}} = \frac{xF}{\xi M_{\text{Ni}_3\text{Sn}}} = 90.92337x/\text{mA} \cdot \text{h/g}, \quad (9)$$

where F is the Faraday constant and ξ is the structural coefficient of materials, and M is the relative molecular weight of the anode materials.

3.2. The analysis of lithium insertion mechanism

The electrochemical parameters and electronic structure of the lithiation interphase $\text{Li}_x\text{Ni}_3\text{Sn}$ (x = 0, 0.5, 1, 1.5, 2, 2.5) are calculated using CASTEP software package. The partial results are described in Table1, Fig.2 and Fig.3. Meanwhile, phases $\text{Li}_3\text{Ni}_3\text{Sn}_2$, $\text{Li}_3\text{Ni}_3\text{Sn}_4$ are added for comparison.

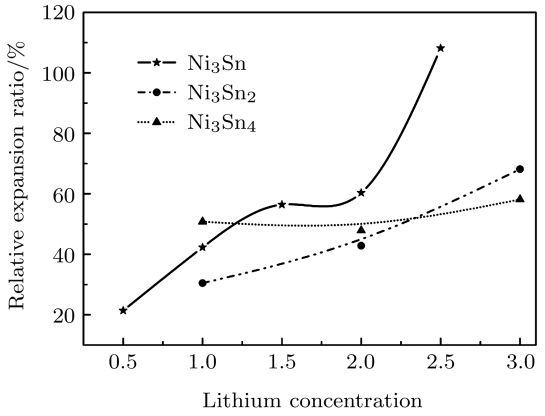


Fig.2. Relative expansion ratio as a function of lithium concentration for Sn–Ni alloy phases.

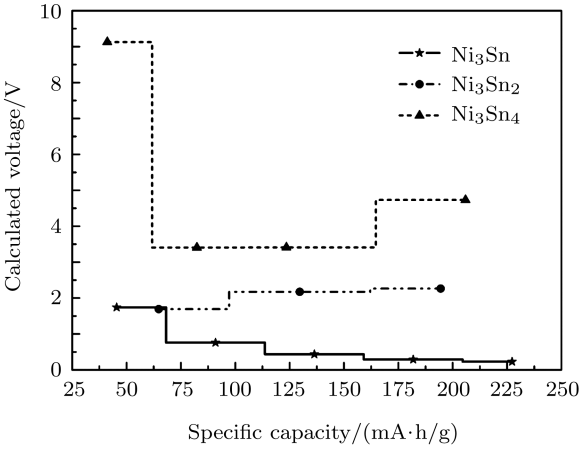


Fig.3. Calculated electrochemical voltage as function of specific capacity for Sn–Ni alloy phases.

From Table 1 and Fig.2, we can find that the relative expansion ratio increases gradually with the content of lithium insertion in Sn–Ni alloy phases. Under the same lithium intercalation, compared with other stable phases Ni_3Sn_2 and Ni_3Sn_4, Ni_3Sn has larger relative expansion ratio. This phenomenon indicates that the lithium atoms inhabit the interstitial sites of the host materials Ni_3Sn. Furthermore, according to Fig.2, we find that the relative volume expands dramatically when the Li concentration is greater than

Table 1. Total energy, average voltage, relative expansion ratio and specific capacity for Sn–Ni alloy interphases.

samples	total energy /Li_xNi_3Sn/eV	average voltage/V	$Li_xNi_3Sn/10^{-3}nm^3$	expansion ratio/%	capacity/(mA·h/g)
Ni_3Sn	–4175.7790	–	51.0148	–	–
$Li_{0.5}Ni_3Sn$	–4261.0796	1.74217	61.9325	21.4010	45.4617
$LiNi_3Sn$	–4356.2236	0.75782	72.5827	42.2780	90.9234
$Li_{1.5}Ni_3Sn$	–4451.3144	0.43325	79.7862	56.3981	136.3851
Li_2Ni_3Sn	–4546.0215	0.29015	81.7882	60.3224	181.8467
$Li_{2.5}Ni_3Sn$	–4640.1631	0.22691	106.1979	108.1706	227.3084
$Li_3Ni_3Sn_2$	–4833.3025	2.26310	128.1643	68.1589	194.4626
$Li_3Ni_3Sn_4$	–5025.8214	3.40960	175.8224	40.6660	123.5338

$x = 2$, at which the octahedral interstitial sites just are fully filled due to the lithium atoms jammed the host material, and then lithium atoms will further inhabit the tetrahedral interstitial sites in the subsequent charge process. The maximum value occurs at $x = 2.5$ when two kinds of interstitial sites are filled synchronously and the maximum expansion ratio is 108.1706%.

Also we find that in order to stabilize the morphology of Sn–Ni alloy electrode, the interphase Ni_3Sn must keep a small volume effect during the process of electrochemical reaction so as to prevent the cracking and pulverization of electrode, and eventually provide a good structural and cyclic performance for the electrode material. As a result, that interphase will gradually deteriorate the Sn–Ni alloy electrode, especially when tetrahedral interstitial sites are jammed by the lithium atoms, which make the crystal structure of intermetallic lithiation compounds expand and distort heavily in the process of deeply charging. Due to the octahedral interstitial sites are prone to lithium insertion than that of tetrahedral interstitial sites, the relative expansion ratio is small when lithium atoms are only inhabited in octahedral interstitial sites.

The true equilibrium voltage profile would be single value with respect to charge and discharge. Since the experiment is not performed at an infinitesimally slow rate, the actual equilibrium voltage profile is not been measured. According to the equations (7) and (9), calculated electrochemical voltage as function of specific capacity for Sn–Ni alloy phases is showed in Fig.3. It is obviously that the electrochemical voltage of Li_xNi_3Sn alloy phase is lower than that of other phases under the same lithium intercalation. Its specific capacity increases with the decreasing electrochemical voltage, and the change trend is in good agreement with the first charging–discharging experimental curves of Sn–Ni alloy. The calculated capacity reaches up to 227.31 $mA \cdot h/g$ for Li_xNi_3Sn alloy with $x = 2.5$. The voltage plateaus occur when lithium atoms inhabit all octahedral interstitial sites and lithium insertion voltage is around 0.3 eV.

3.3. The analysis of electronic structure

The relationships between the total density of states of Li_xNi_3Sn ($x = 0, 1, 2, 2.5$) and partial density of states of lithium, nickel and tin atoms are shown in Fig.4. It can be seen that the orbits of different atoms contribute to the main peak of total density of states. Among them, the 3d orbits of nickel atoms and 5p orbits of tin atoms play the main role, that is, band structure of Li_xNi_3Sn interphase alloys is mainly composed of the 3d orbits of nickel atoms and 5p orbits of tin atoms. And the peak of total density of states of Li_xNi_3Sn interphase near the Fermi energy is mainly offered by the 3d orbits of nickel atoms. Moreover, the peak intensity increases slightly with the lithium intercalation. Consequently, the electrochemical characteristic of nickel atoms is very stable in the charging/discharging process. And Li_xNi_3Sn interphase compounds become the main contributors to the reversible capacity of electrode ascribed to the active tin atoms.

Obviously, from the Figs.4(b)–4(d), the 1s, 2s orbits of lithium atoms have main contribution to the peaks of Li_xNi_3Sn interphase from –47 eV to –44 eV. Meanwhile, the peak shape transforms gradually from double peak to single peak shape, then keeps stability at the range of high energy field. However, the peak shape and intensity of the tin atoms change largely near the Fermi energy, which might be ascribed to

the reaction between the tin atoms and lithium atoms that occurs during charging and discharging process. A turning point appears when the lithium concentration of the Li_xNi_3Sn interphase arrive at 33.3at%, namely, the octahedral interstitial sites just are full filled. The result is consistent with the analysis in the second part.

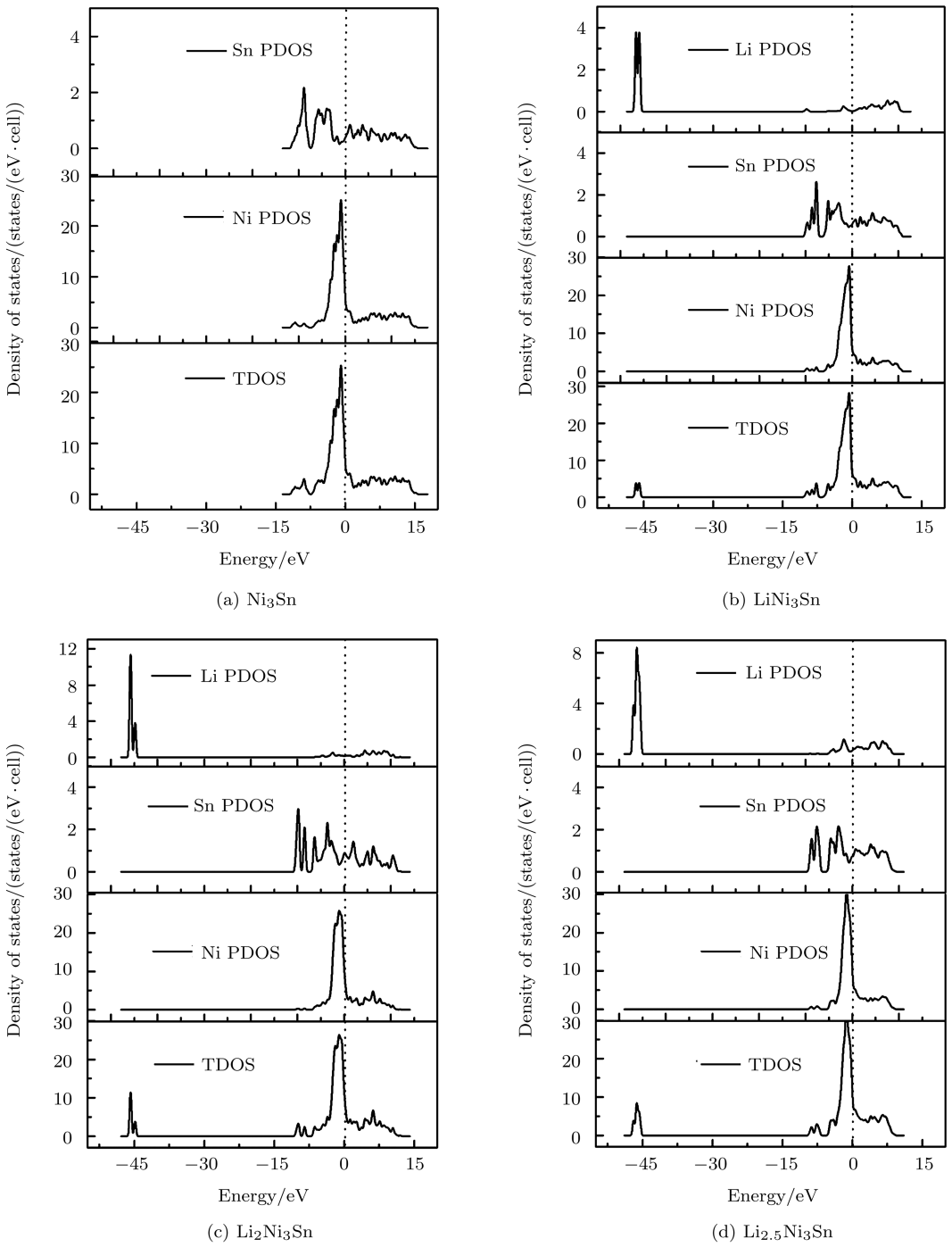


Fig.4. Density of states for Li_xNi_3Sn with $x = 0$, 1, 2, 2.5 respectively (the dot line is Fermi energy).

The relationship between Fermi energy and lithium concentration for Sn–Ni alloy is shown in Fig.5. Compared with Ni_3Sn_2 and Ni_3Sn_4, Ni_3Sn has higher Fermi energy under the same lithium concentration, although other interphases have higher lithium concentration. Since the structural expansion

ratio of various interphases has positive linear relationship with lithium concentration, we can come to conclusion that under the same lithium concentration the interphase whose Fermi energy is higher has large expansion ratio.

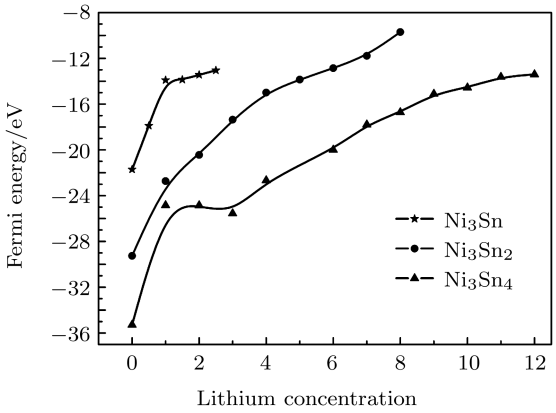


Fig.5. Relationship between Fermi energy and lithium concentration for Sn–Ni alloys.

Consequently, Ni_3Sn has lower theoretical capacity and larger expansion ratio than that of other interphases such as Ni_3Sn_2, Ni_3Sn_4. The technological parameters during preparing the Sn–Ni alloy electrode must be controlled strictly to make the content of Ni_3Sn interphase as low as possible. At the same time, the concentration of lithium atoms must be below the limit capacity of inhabiting octahedral interstitial sites even though the Ni_3Sn interphase appear.

4. Conclusion

In this paper, the plane-wave pseudopotential method is used to calculate the electrochemical parameters and electronic structures of lithium insertion interphases Li_xNi_3Sn (x = 0, 0.5, 1, 1.5, 2, 2.5). The results show that the first-principle investigation can give practical information and insights about the structural stability and electrochemical voltage profile. Ni_3Sn interphase has larger relative expansion ratio and lower electrochemical voltage. Especially, the presence of a turning point when the octahedral interstitial sites are full filled will change greatly the cyclic performance of Sn–Ni alloy electrode. Therefore the investigation of lithium insertion mechanism of various interphases plays an important role in synthesizing practical and effective anode materials.

References

[1] Sato K, Noguchi M, Demachi A, Oki N and Endo M 1994 *Science* **264** 556

[2] Kang K, Meng Y S, Breger J, Grey C P and Ceder G 2006 *Science* **311** 977

[3] Ouyang X F, Shi S Q, Ouyang C Y, Jiang D Y, Liu De S, Ye Z Q and Lei M S 2007 *Chin. Phys.* **16** 3042

[4] Noriyuki T, Ryuji O, Masahisa F, Shin F, Maruo K and Ikuo Y 2002 *J. Power Sources* **107** 48

[5] Mukaibo H, Momma T and Osaka T 2005 *J. Power Sources* **146** 457

[6] Li H, Huang X J, Chen L Q, Wu Z G and Liang Y 1999 *Electrochem. Solid-State Lett.* **2** 47

[7] Park M S, Rajendran S, Kang Y M, Han K S, Han Y S and Lee J Y 2006 *J. Power Source* **158** 650

[8] Ceder G, Chiang Y M, Sadoway D R, Aydinol M K, Jang Y I and Huang B 1998 *Nature* **392** 694

[9] Wolverton C and Zunger A 1998 *Phys. Rev. Lett.* **81** 606

[10] Shi S Q, Ouyang C Y, Wang D S, Chen L Q and Huang X J 2003 *Solid State Commun.* **126** 531

[11] Tian X Q, Du S X and Gao H J 2008 *Chin. Phys.* B **17** 0286

[12] Xu Y N, Chung S Y, Bloking J T, Chiang Y M and Ching W Y 2004 *Electrochem. Solid-State Lett.* **7** A131

[13] Tang P and Holzwarth N A W 2003 *Phys. Rev.* B **68** 165107

[14] Courtney I A, Tse J S, Mao O, Hafner J and Dahn J R 1998 *Phys. Rev.* B **58** 15583

[15] Kganyago K R, Ngoepe P E and Catlow C R A 2003 *Solid State Ionics* **159** 21

[16] Yan J, Su Y C, Su J T and Lu P T 2006 *Trans. Nonferrous Met. Soc. China* **16** 1380

[17] Chen K, Fan G H and Zhang Y 2008 *Acta Phys. Sin.* **57** 1054 (in Chinese)

[18] Hou X H, Hu S J, Li W S, Zhao L Z, Yu H W and Tan C L 2008 *Acta Phys. Sin.* **57** 2374 (in Chinese)

[19] Segall M D, Lindan P J D, Probert M J, Pickard C J, Hasnip P J, Clark S J and Payne M C 2002 *J. Phys.* **14** 2717

[20] Perdew J P, Chevary J A, Vosko S H, Jackson K A, Pederson M R, Singh D J and Fiolhais C 1992 *Phys. Rev.* B **46** 6671

[21] Vanderbilt D 1990 *Phys Rev.* B **41** 7892

[22] Monkhorst H J and Pack D 1976 *Phys. Rev.* B **13** 5188

[23] Xu B, Cheng Z Z, Yi L and Cheng Z 2007 *Chin. Phys.* **16** 3798

[24] Aydinol M K, Kohan A F, Ceder G, Cho K and Joannopoulos J 1997 *Phys. Rev.* B **56** 1354

[25] Shi S Q, Wang D S, Meng S, Chen L Q and Huang X J 2003 *Phys. Rev.* B **67** 115130